ChemComm

Accepted Manuscript

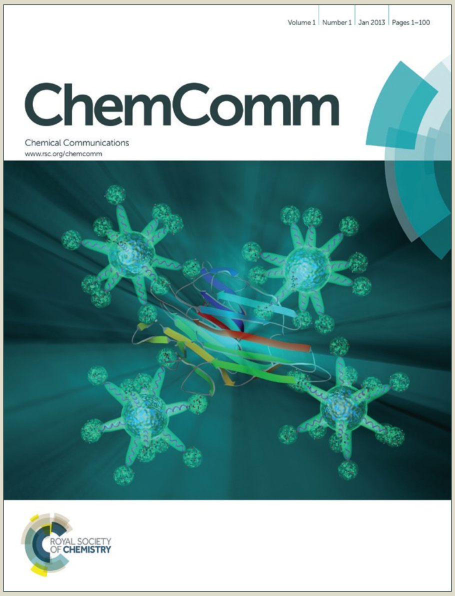

ROYAL SOCIETY OF CHEMISTRY

www.rsc.org/chemcomm

Journal Name RSCPublishing

COMMUNICATION

Magnetocaloric Effect and Thermal Conductivity of $Gd(OH)_3$ and $Gd_2O(OH)_4(H_2O)_2$†

Cite this: DOI: 10.1039/x0xx00000x

Yan Yang, Qian-Chong, Zhang, Yin-Yin Pan, La-Sheng Long* and Lan-Sun Zheng

Received 00th January 2012,
Accepted 00th January 2012

DOI: 10.1039/x0xx00000x

www.rsc.org/

Magnetocaloric effect (MCE) and thermal conductivity of two gadolinium hydroxides, $Gd(OH)_3$ (1) and $Gd_2O(OH)_4(H_2O)_2$ (2) are investigated. Magnetic study indicates that both 1 and 2 exhibit antiferromagnetic interaction, and the MCE for 1 and 2 at 2 K and ΔH = 7 is 62.00 J kg^{-1} K^{-1} and 59.09 J kg^{-1} K^{-1}, respectively. Investigation on their thermal conductivity shows that the thermal conductivity for 1 is significantly better than that for 2.

Since the magnetocaloric effect (MCE) was discovered by Warburg in 1881,[1] magnetic refrigeration, a cooling technology based on the MCE,[2] has attracted much interest in the field of magnetic materials,[3] due to its environmental friendliness and energy efficiency.[3b] Among different types of magnetic materials, metal clusters and coordination polymers are especially notable. On one hand, their structural diversity and controllability facilitate us to adjust the magnetic interaction between the metal ions, leading to their MCE significantly larger than that of lanthanide alloys and magnetic nanoparticles;[4,5] On the other hand, using this kind of magnetic materials as magnetic reagents can achieve ultra-low temperature,[3d] due to their magnetic phase transition often occurring at extremely low temperature.[4-6] In the past decades, a lot of metal clusters and coordination polymers, such as, $\{Mn_{12}\}$,[7] $\{Fe_8\}$,[8] $\{Mn_4Gd_4\}$,[9] $\{Gd_{36}Ni_{12}\}$,[10] $\{Gd_{42}Co_{10}\}$,[11] $\{Gd_2\}$,[12] $[Gd(HCOO)_3]_n$,[4] $[Gd(OH)CO_3]_n$,[5] $[Gd_2(OH)_2(suc)_2(H_2O)]_n\cdot 2nH_2O$[13] and $[Gd_6(OH)_8(suc)_5(H_2O)_2]_n\cdot 4nH_2O)$,[13] have been prepared. However, the application of the magnetic reagents, especially in ultra-low temperature, remains a great challenge. The obstacle to the application of the magnetic reagents is mainly attributed to the following two reasons, one is that the magnetic entropy of the magnetic materials synthesized so far is not large enough, leading to small temperature change in each a refrigeration cycle; Another is that the thermal conductivity of the magnetic materials synthesized so far is not good enough, decreasing the thermal efficiency of the refrigeration cycle. To our surprise, although great many efforts have been made to investigate the MCE of the materials, study on their thermal conductivity is seldom recognized.

Gadolinium hydroxides (for an example, $Gd(OH)_3$), possessing large metal/ligand ratio, are expected to have a large MCE. Theoretical calculation based on $nR\ln(2S+1)/Mw$ reveals that the MCE ($-\Delta S_m$) of $Gd(OH)_3$ can be up to 83.01 J kg^{-1}K^{-1}.[10] More importantly, gadolinium hydroxides often crystallize in high symmetric space group ($P6_3/m$),[14] and thus they may have good thermal conductivity, because thermal conductivity of non-metallic compounds is closely related to their structural symmetry.[15] Considered the fact that the magnetic order temperature of gadolinium hydroxides is extremely low,[6] it is expected that gadolinium hydroxides are good candidates for ultra-low temperature magnetic reagents. Along this line, we respectively use Gd_2O_3 and $Gd(NO_3)_3$ to synthesize gadolinium hydroxides, and report herein the MCE and thermal conductivity of two gadolinium hydroxides, namely, $Gd(OH)_3$ (**1**) and $Gd_2O(OH)_4(H_2O)_2$ (**2**).

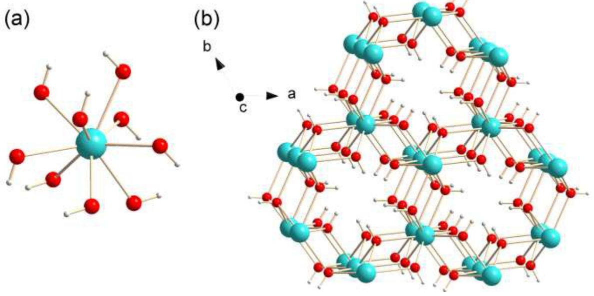

Fig. 1 (a) The coordination environment of Gd^{3+}. (b) The 3D structure of **1**. Gd: cyan, O: red. H: light gray.

Compound **1** was obtained through hydrothermal reaction of Gd_2O_3 and NaOH,† instead of the early reported method which needs to dissolved Gd_2O_3 in HNO_3.[16] Single-crystal structure of **1** reveals that it crystallizes in hexagonal space group $P6_3/m$, in accord with previous research by G. W. Beall and his co-workers.[14] Each asymmetric unit in **1** consists of 1/6 Gd^{3+} ion and 1/2 OH^- ion. Each Gd^{3+} ion coordinated with nine μ_3-OH^- in tetrakaidecahedron geometry (Fig. 1a), and each OH^- group bridging to three Gd^{3+} ions generates a 3D structure with 1D hexagram channel as shown in Fig. 1b. The bond lengths of Gd-O are in the range from 2.437 to 2.452 Å, the bond angles of Gd-O-Gd are 95.4° to 112.3°, while the separations of Gd···Gd are 3.606 Å and 4.059 Å respectively.

Compound **2** was obtained through hydrothermal reaction of $Gd(NO_3)_3{\cdot}6H_2O$, $HCOONa{\cdot}2H_2O$ and glycine.† It was mentioned that the HCOONa and glycine play an important role in the synthesis. Without the HCOONa and glycine, it is impossible to adjust the pH value of the reaction to 6.7. Single-crystal structure analysis reveals that **2** crystallizes in orthorhombic, space group *Cmcm*. The asymmetric unit in **2** consists of 1 Gd^{3+} ion, 1/2 O^{2-} ion, 2 OH^- ions and one coordination water molecule. There are two crystallography independent Gd^{3+} ions (Gd1 and Gd2) in **2**. The Gd1 is eight-coordinated with six μ_3-OH^-, one μ_3-O^{2-} and one H_2O in dodecahedron geometry, and the Gd2 is nine-coordinated with six μ_3-OH^-, two μ_3-O^{2-} and one H_2O in tetrakaidecahedron geometry. The existence of the O^{2-} in **2** can be demonstrated from its average Gd-O distance and the hydrogen-bonding interaction between the O^{2-} and coordination water molecules, in addition to the charge balance. In **2**, the average Gd-O distance for the O^{2-} is 2.390 Å, significantly shorter than that of 2.418-2.5223 Å for the OH^-. Consistently, if taking the μ_3-O^{2-} in **2** as μ_3-OH^-, the hydrogen-bonding interaction between the μ_3-OH^- and coordinated water will be unreasonable, because the distance between H atom in OH^- and the H atom in coordinated water is only about 1.9 Å.

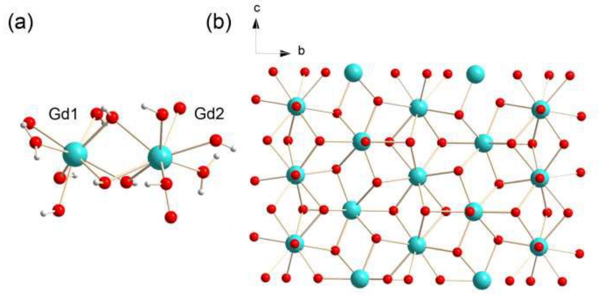

Fig. 2 (a) The coordination environment of Gd^{3+} in **2**. (b) The 2D structure in **2** viewed along the *a* axis. Gd: cyan, O: red, H: light gray. H atoms in (b) are omitted for clarity.

The 2D structure in **2** can viewed as connection of adjacent Gd2 ions through two OH^- and one O^{2-} bridges, adjacent Gd1 ions through two OH^- bridges and adjacent Gd1 and Gd2 ions through three OH^- bridges as shown in Fig. 2b. The adjacent 2D structures connected through hydrogen-bonding interaction between the coordination water molecules from adjacent 2D structures generates a 3D structure of **2** (ESI, Fig. S1). The bond lengths of Gd-O are in the range from 2.324 to 2.617 Å. The bond angles of Gd-O-Gd are in the range from 93.2 to 111.3° and the Gd···Gd separations are in the range from 3.655 to 3.939 Å. These values are comparable to the corresponding values in **1**.

The temperature dependence of the magnetic susceptibility for **1** and **2** was measured from 2 to 300 K in an applied magnetic field of 1000 Oe respectively. As shown in Fig. S2 (ESI), the $\chi_M T$ for **1** at 300 K is 8.00 $cm^3 \cdot K \cdot mol^{-1}$, close to that of 7.88 $cm^3 \cdot K \cdot mol^{-1}$ calculated for one Gd^{3+} ion (S = 7/2, g = 2). The $\chi_M T$ for **2** at 300 K is 15.51 cm^3 K mol^{-1}, close to that of 15.75 cm^3 K mol^{-1} calculated for two non-interacting Gd^{3+} ions. With decreasing temperature, the $\chi_M T$ for **1** and **2** remains essentially constant and then decreases gradually from 100 K to 30 K. On further lowering the temperature, the $\chi_M T$ drops abruptly, and reaches 3.32 cm^3 K mol^{-1} for **1** and 5.83 cm^3 K mol^{-1} for **2** at 2 K, suggesting existence of antiferromagnetic coupling in **1** and **2**. Consistently, fitting the data in the range of 50-300 K with Curie-Weiss law yields $C = 8.18$ cm^3 K mol^{-1}, $\theta = -1.69$ K for **1** and $C = 15.84$ cm^3 K mol^{-1}, $\theta = -4.58$ K for **2**. The overall magnetic coupling characterized by the Weiss constant for **1** and **2** further confirms the antiferromagnetic coupling in **1** and **2**.

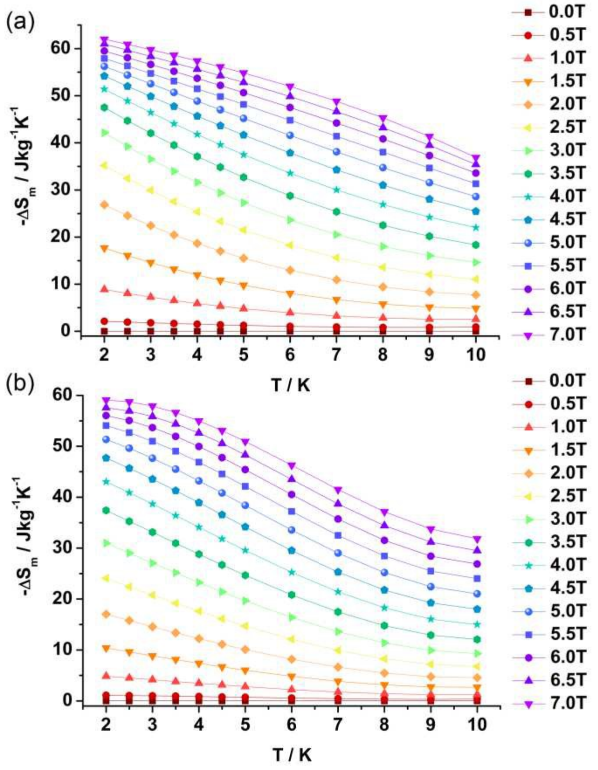

Fig. 3 Values of −ΔS m calculated using the magnetization data for **1** (a) and **2** (b) at various fields and temperatures.

Measurements of the field-dependent the magnetizations of **1** and **2** at low temperature (2-10 K) were also performed (ESI, Fig. S3). The magnetization for **1** and **2** increases steadily with the applied field and reaches 6.99 $N\mu_B$ for **1** and 13.65 $N\mu_B$ for **2** at 2 K and 7 T, in agreement with the calculated value of 7 $N\mu_B$ for **1** and 14 $N\mu_B$ for **2** respectively. Based on these data, the magnetic entropy change, a key parameter in evaluating the MCE, can be obtained by applying the equation of $\Delta S_m(T)_{\Delta H} = \int[\partial M(T, H)/\partial T]_H \, dH$.[11] As shown in Fig. 3, the $-\Delta S_m$ for **1** and **2** at 2 K and $\Delta H = 7$ T is 62.00 J kg^{-1} K^{-1} (346.08 mJ cm^{-3} K^{-1}) and 59.09 J kg^{-1} K^{-1} (216.86 mJ cm^{-3} K^{-1}) respectively. The $-\Delta S_m$ for **1** and **2** smaller than the theoretical limiting value of $-\Delta S_m = 83.01$ J kg^{-1} K^{-1} (463.36 mJ cm^{-3} K^{-1}) for **1** and 79.57 J kg^{-1} K^{-1} (292.02 mJ cm^{-3} K^{-1}) for **2** calculated by using the equation $-\Delta S_m = nR\ln(2s+1)/Mw$ is attributed to the presence of antiferromagnetic interaction in **1** and **2**.[10] It was mentioned that the gravimetric entropy change larger than 50 J kg^{-1} K^{-1} at 2 K and $\Delta H =$ 7 T has only been observed in four compounds (Tab. 1),[4,5,17,18] while the volumetric entropy change larger than 210 mJ cm^{-3} K^{-1} has only observed in three compounds so far (including in the commercial magnetic refrigerant GGG[19]), despite a great many efforts made. Based on the Tab. 1, it is clear that $-\Delta S_m$ for **1** at 2 K and ΔH = 7 T is comparable to that of 66.4 J kg^{-1} K^{-1} (355 mJ cm^{-3} K^{-1}) at 1.8 K and ΔH = 7 T, the largest $-\Delta S_m$ reported so far,[5] while the $-\Delta S_m$ for **2** at 2 K and ΔH = 7 T is comparable to that of 55.9 J kg^{-1} K^{-1} (216 mJ cm^{-3} K^{-1}) in $Gd(HCOO)_3$.[4]

Significantly, MCE for **1** can also get satisfying value of 26.9 J kg^{-1} K^{-1} (150 mJ cm^{-3} K^{-1}) at ΔH = 2 T. This value is significantly larger than that for the GGG ($-\Delta S_m \approx$ 14.6 J kg^{-1} K^{-1}, 105 mJ cm^{-3} K^{-1}, at ΔH = 2 T),[19] indicating that **1** is a promising magnetic refrigeration materials. It was mentioned that, although the ΔS_m for **1** at 2 K and ΔH = 7 T is comparable to that for **2** at 2 K and ΔH = 7 T, the ΔS_m for **1** at 2 K and ΔH = 2 T is significantly larger than that for **2** (ΔS_m = 17.0 J kg^{-1} K^{-1}, 62 mJ cm^{-3} K^{-1}) at 2 K and ΔH = 2 T, revealing the weaker the antiferromagnetic interaction in the compound, the larger the MCE at low magnetic field.

Tab. 1 Magnetic Entropy Change for Selected Materials

Compound[ref]	ΔH (T)	$-\Delta S_{m,max}$ (J kg^{-1} K^{-1})	$-\Delta S_{m,max}$ (mJ cm^{-3} K^{-1})
{[Mn $(H_2O)_6$] [MnGd-$(oda)_3]_2\cdot 6H_2O\}_n$[17]	7	50.1	114
	2	35.2	80
[Gd $(HCOO)_3]_n$[4]	7	55.9	216
	2	12.3	48
[Mn $(glc)_2(H_2O)_2]$[18]	7	60.3	112
	2	34.9	65
[Gd $(OH)CO_3]_n$[5]	7	66.4	355
	2	32.4	173
GGG	7	38.3	273
	2	14.6	105
1 in this work	7	62.0	346
	2	26.9	150
2 in this work	7	59.1	217
	2	17.0	62

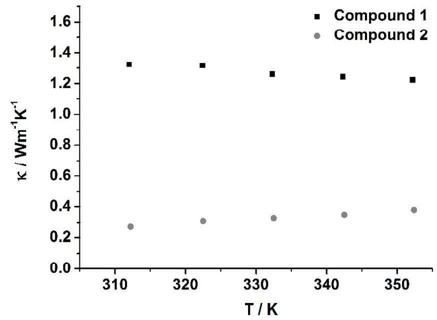

Fig. 4 Temperature-dependent thermal conductivity for **1** and **2**.

Because thermal conductivity property of the materials plays a key role in enhancing the thermal efficiency of the refrigeration cycle, the thermal conductivity for **1** and **2** was investigated respectively, so as to evaluate **1** and **2** as magnetic refrigeration materials. Based on the equation of $\kappa = \alpha c_p \rho$ for non-metal materials[20] (where α is thermal diffusion coefficient, c_p is specific heat capacity, and ρ is the density of the materials), it is clear that thermal conductivity for a given non-metal material is proportional to its thermal diffusion coefficient, specific heat capacity and density respectively. As the density of **1** and **2** could be obtained from their crystal structures, thus, the thermal diffusion coefficient and the specific heat capacity of **1** and **2** were investigated respectively in the temperature range from 312 to 352 K, due to equipment limited. As shown in Fig. S4 (ESI), the specific heat capacity for **1** at 312 K is 0.58 J g^{-1} K^{-1}. With increasing temperature, the specific heat capacity for **1** remains essentially constant and reaches 0.61 J g^{-1} K^{-1} at 352 K. In contrast, the specific heat capacity for **2** is significantly affected with the temperature, and it changes from 0.53 J g^{-1} K^{-1} at 312 K to 0.71 J g^{-1} K^{-1} at 352 K.

Fig. S5 (ESI) illustrated the thermal diffusion coefficient for **1** and **2** measured in the temperature range from 312 to 352 K. With the increase of temperature, the thermal diffusion coefficient for **1** decreases gradually, and reaches 0.41 mm^2 s^{-1} at 312 K. However, the thermal diffusion coefficient for **2** increases with the decrease of the temperature and reaches 0.14 mm^2 s^{-1} at 312 K. The thermal diffusion coefficient for **1** significantly better than that for **2** is attributed to the symmetry in **1** higher than that in **2**.[15]

Fig. 4 illustrated temperature-dependent thermal conductivity of **1** and **2**. The thermal conductivity for **1** increases with the decrease of temperature, while this for **2** decreases with the decrease of the temperature in the temperature range from 312 to 352 K. At 312 K, the thermal conductivity for **1** and **2** is 1.32 and 0.27 W M^{-1} K^{-1} respectively. It was noted that the thermal conductivity of **1** at 312 K is in the same order of magnitude as that of the GGG (9 W m^{-1} K^{-1})[19] at room temperature. Because of both the ΔS_m and the thermal conductivity of **1** significantly larger than that of **2**, the thermal conductivity of **1** in the low temperature range was further investigated theoretically according to the reported method,[21] due to the equipment limited. Based on the specific heat capacity of **1** measured in the temperature range from 100 to 400 K and the low temperature specific heat of **1** in the temperature range from 0.43 to 5.1 K reported previously,[6] the thermal conductivity of **1** at 0.93 K (the magnetic order temperature of **1**) is about 4.45 W m^{-1} K^{-1} (ESI). Although this value is significantly smaller than that of about 9 W m^{-1} K^{-1} at 3 K for GGG measured through its single-crystal,[22] considered the fact that the thermal conductivity of a given material measured through its powder sample would be significantly smaller than that measured through its single-crystal,[23] it is reasonable to conclude that **1** is a promising candidate for ultra-low temperature magnetic refrigeration material.

Conclusions

In this study, we have reported the magnetocaloric effect and thermal conductivity of two gadolinium hydroxides, **1** and **2**. Study on their MCE at 2 K and ΔH = 2 T indicates that the ΔS_m for **1** is significantly larger than that for **2**, demonstrating the weaker the antiferromagnetic interaction in the compound, the larger the MCE at low magnetic field. Investigation on their thermal conductivity shows that the thermal conductivity for **1** is significantly better than that for **2**, revealing that high symmetry of the compound will enhance its thermal conductivity. Considered the fact that MCE for **1** at ΔH = 2 T is significantly larger than that for the GGG and the thermal conductivity of **1** at 0.94 K is up to 4.45 W m^{-1} K^{-1}, **1** will be the most promising candidate for ultra-low temperature magnetic refrigeration reagent reported so far.

This work was supported by the 973 project from MSTC (grant no. 2012CB821704 and 2014CB84561), and the NNSFC (grant nos. 21431005 and 21390391) for financial support.

Notes and references

Collaborative innovation center of chemistry for energy materials, State Key Laboratory of Physical Chemistry of Solid Surface and Department of Chemistry, College of Chemistry and Chemical Engineering, Xiamen University, Xiamen 361005, China. Fax: (+)86-592-218-3047; Tel:(+) 86-592-2189638; E-mail: lslong@xmu.edu.cn

† **Synthesis of 1**: Gd_2O_3 (0.363 g, 1 mmol) was dissolved in freshly prepared aqueous solution of NaOH (10 mL, 20 mol·L^{-1}). The resulting mixture was transferred to a Parr Teflon-lined stainless-steel vessel (23 mL). The vessel was heated to 250 ºC over a period of 300 min, and maintained at that temperature for 4000 min, then cooled to room temperature. Colourless crystals were obtained in 91.1 % yield (based on Gd). C, H, N analysis (%) calculated for GdH_3O_3 (FW = 208.27) was: C 0, H 1.45, N 0; the experimental analysis was: C 0.041, H 1.52, N 0.043. IR date (KBr, cm^{-1}): 3437 (s), 1630 (w), 1051(w), 698 (s).

† **Synthesis of 2**: $Gd(NO_3)_3·6H_2O$ (0.113 g, 0.25 mmol), $HCOONa·2H_2O$ (0.034 g, 0.33 mmol) and glycine (0.006 g, 0.08 mmol) were dissolved in deionized water (15 mL). A freshly prepared aqueous solution of $NH_3·H_2O$ (1.0 mol·L^{-1}) was added dropwise to adjust the pH of the solution to 6.7 while stirring. The resulting mixture was transferred to a Parr Teflon-lined stainless-steel vessel (23 mL). The vessel was heated to 160 ºC over a period of 250 min, and maintained at that temperature for 4000 min, then cooled to room temperature over a period of 4000 min. Colourless crystals were obtained in 23.2 % yield (based on Gd). C, H, N analysis (%) calculated for $Gd_2H_8O_7$ (FW = 434.56) was: C 0, H 1.85, N 0; the experimental analysis was: C 0.11, H 1.92, N 0.15. IR date (KBr, cm^{-1}): 3435 (s), 1630 (s), 1383 (s), 1047 (w), 644 (s).

Materials and methods: All reagents and solvents were commercially available and used as received. The C, H and N microanalyses were carried out with a CE instruments EA 1110 elemental analyzer. The infrared spectrum was recorded on a Nicolet AVATAR FT-IR330 spectrophotometer with KBr pellets in the range of 4000-400 cm^{-1}. Magnetic susceptibility was measured by a Quantum Design MPMS superconducting quantum interference device (SQUID). The specific heat capacity measurement was performed on the NETZSCH DSC 200F3 under nitrogen atmosphere from 312 K to 352 K with sweeping rate of 10 K min^{-1}. Thermal conductivity was measured on NETZSCH LFA457/2/G by laser flash method under nitrogen atmosphere in the temperature range of 312-352 K.

† Electronic Supplementary Information (ESI) available: [The 3D structure of **2**, the temperature dependence of the magnetic susceptibility, field-dependent magnetization, specific heat capacity, thermal diffusion coefficient for **1** and **2**, the calculation of thermal conductivity of **1** at low temperature, and Single-crystal X-ray structure determination of **1** and **2**]. See DOI: 10.1039/b000000x/

1 E. Warburg, *Ann. Phys.*, 1881, **249**, 141.
2 V. K. Pecharsky, K. A. Gschneidner Jr, *J. Magn. Magn. Mater.*, 1999, **200**, 44.
3 (a) J. A. Barclay, W. A. Steyert, *Cryogenics*, 1982, **22**, 73; (b) K. A. Gschneidner Jr, V. K. Pecharsky, *Int. J. Refrig.*, 2008, **31**, 945; (c) B. G. Shen, J. R. Sun, F. X. Hu, H. W. Zhang, Z. H. Cheng, *Adv. Mater.*, 2009, **21**, 4545; (d) Y. Z. Zheng, G. J. Zhou, Z. Zheng, R. E. P. Winpenny, *Chem. Soc. Rev.*, 2014, **43**, 1462; (e) L. Sedláková, J. Hanko, A. Orendáčová, M. Orendáč, C. L. Zhou, W. H. Zhu, B. W. Wang, Z. M. Wang, S. Gao, *J. Alloys Compd.*, 2009, **487**, 425.
4 G. Lorusso, J. W. Sharples, E. Palacios, O. Roubeau, E. K. Brechin, R. Sessoli, A. Rossin, F. Tuna, E. J. L. McInnes, D. Collison, M. Evangelisti, *Adv. Mater.*, 2013, **25**, 4653.
5 Y. C. Chen, Z. S. Meng, L. Qin, Y. Z. Zheng, J. L. Liu, F. S. Guo, R. Tarasenko, M. Orendáč, J. Prokleška, V. Sechovsky´, M. L. Tong, *J. Mater. Chem. A.*, 2014, **2**, 9851.
6 A. T. Skjeltorp, C. A. Catanese, H. E. Meissner, W. P. Wolf, *Phys. Rev. B.*, 1972, **7**, 2062.
7 F. Torres, J. M. Hernández, X. Bohigas, J. Tejada, *Appl. Phys. Lett.*, 2000, **77**, 3248.
8 X. X. Zhang, H. L. Wei, Z. Q. Zhang, L. Zhang, *Phys. Rev. Lett.*, 2001, **87**, 157203.
9 G. Karotsis, M. Evangelisti, S. J. Dalgarno, E. K. Brechin, *Angew. Chem. Int. Ed.*, 2009, **48**, 9928.
10 J. B. Peng, Q. C. Zhang, X. J. Kong, Y. P. Ren, L. S. Long, R. B. Huang, L. S. Zheng, Z. Zheng, *Angew. Chem. Int. Ed.*, 2011, **50**, 10649.
11 J. B. Peng, Q. C. Zhang, X. J. Kong, Y. Z. Zheng, Y. P. Ren, L. S. Long, R. B. Huang, L. S. Zheng, Z. Zheng, *J. Am. Chem. Soc.*, 2012, **134**, 3314.
12 M. Evangelisti, O. Roubeau, E. Palacios, A. Camón, T. N. Hooper, E. K. Brechin, J. J. Alonso, *Angew. Chem. Int. Ed.*, 2011, **50**, 6606.
13 Y. C. Chen, F. S. Guo, Y. Z. Zheng, J. L. Liu, J. D. Leng, R. Tarasenko, M. Orendáč, J. Prokleška, V. Sechovský, M. L. Tong, *Chem. Eur. J.*, 2013, **19**, 13504.
14 G. W. Beall, W. O. Milligan, H. A. Wolcott, *J. Inorg. Nucl. Chem.*, 1977, **39**, 65.
15 J. F. Nye *in Physical Properties of Crystals*, Clarendon Press, Oxford, 1957. pp. 322.
16 S. Mroczkowski, J. Eckert, H. Meissner, J. C. Doran, *J. Cryst. Growth.*, 1970, **7**, 333.
17 F. S. Guo, Y. C. Chen, J. L. Liu, J. D. Leng, Z. S. Meng, P. Vrábel, M. Orendáč, M. L. Tong, *Chem. Commun.*, 2012, **48**, 12219.
18 Y. C. Chen, F. S. Guo, J. L. Liu, J. D. Leng, P. Vrábel, M. Orendáč, J. Prokleška, V. Sechovský, M. L. Tong, *Chem. Eur. J.*, 2014, **20**, 3029.
19 (a) G. A. Sack, D. W. Oliver, *Phys. Rev. B.*, 1971, **4**, 592; (b) B. Baudun, R. Lagnier, B. Salce, *J. Magn. Magn. Mater.*, 1982, **27**, 315.
20 (a) W. J. Parker, R. J. Jenkins, C. P. Butler, G. L. Abbott. *J. Appl. Phys.*, 1961, **32**, 1679; (b) R. Endo, T. Yagi, M. Ueda, M. Susa. *ISIJ Int.*, 2014, **54**, 2084.
21 R. Gaumé, B. Viana, D. Vivien, J. Roger, D. Fournier, *Appl. Phys. Lett.*, 2003, **83**, 1355.
22 G. A. Slack, D. W. Olivet, *Phys Rev* 1971, **4B**, 592.
23 J. A. Barclay, S. S. Rosenblum, W. A. Steyert, *Cryogenics* 1976, **16** 539; J. A. Barclay, L. Paterson, D. Bingham, O. Moze, *Cryogenics*, 1978, **18**, 535.